Chem. Senses 34: 425–433, 2009

doi:10.1093/chemse/bjp016
Advance Access publication April 10, 2009

An Odor Stimulator Controlling Odor Temporal Pattern Applicable in Insect Olfaction Study

Koutaroh Okada and Masayuki Sakuma

Division of Applied Biosciences, Graduate School of Agriculture, Kyoto University, Kitashirakawa, Sakyo-ku, Kyoto 606-8502, Japan

Correspondence to be sent to: Masayuki Sakuma, Division of Applied Biosciences, Graduate School of Agriculture, Kyoto University, Kitashirakawa, Sakyo-ku, Kyoto 606-8502, Japan. e-mail: sakuma@kais.kyoto-u.ac.jp

Abstract

The olfactory system of an insect brain codes for information about odorant quality and quantity using the temporal pattern of neural activity as well as neurons' firing. Although an accurate odor temporal pattern is indispensable for investigations of olfactory systems, it is difficult to control in conventional odor stimulators. To overcome this problem, we fabricated an odor stimulator that can control the odor temporal pattern. The stimulator has 3 major parts: an "odor conditioner," with odor-laden air prepared with known concentrations of odorants; a Pitot tube; and a small wind tunnel of laminar flow. Using this stimulator, we realized not only timing control of the odor stimulation with millisecond order but also constant odor concentrations or intensity of stimulation, with error of 2.4% in replicated trials.

Key words: laminar flow, odor concentration, photoionization detector, PIC, Pitot tube, wind tunnel

Introduction

Many neural systems in animals use temporal coding mechanisms to process visual, auditory, tactile, and olfactory stimuli (Fuster and Jervey 1982; Hamilton and Kauer 1988; Laurent and Davidowitz 1994; Meister 1996; Wehr and Laurent 1996; Machens et al. 2001; Nagarajan et al. 2002; Jones et al. 2004; Arabzadeh et al. 2005). In olfactory system studies, mechanisms of odor information coding exploiting temporal parameters have been proposed, such as ensemble coding (Christensen et al. 2000; Stopfer et al. 2003; Lei et al. 2004; Brown et al. 2005). Furthermore, it is known that the temporal pattern of odor concentration strongly affects the response pattern on olfactory receptor cells, neurons in the central nervous system, and behavioral responses in insects (Baker et al. 1988; Christensen et al. 1996; Heinbockel et al. 1999; Vickers et al. 2001; Barrozo and Kaissling 2002). Because temporal coding mechanisms in the insect brain have been widely studied, control of the temporal pattern of stimuli has become a particularly important issue.

Experimental approaches by which odor stimulation has been applied to study olfactory responses in central nervous system by a puff or by mixing of the airborne odor with a continual airflow are numerous. However, the puff and continual airflow methods evoke turbulence. It is generally difficult to know how the odor travels (Vetter et al. 2006) and exactly when odor stimulation starts. In contrast, wind tunnels, which have been widely applied to insect behavior experiments, can control the temporal parameters of odor stimulation (Willis and Baker 1984; Mafra-Neto and Cardé 1995). Because these wind tunnels were designed for behavioral analysis, their size was much larger than the insect itself and odor release site. In a physiological experiment using such a wind tunnel as an odor delivery system, however, relatively large experimental apparatus in a tunnel may generate a turbulent flow (Vetter et al. 2006).

Recently, wind tunnel methods have also been applied to the studies of insect olfactory systems coupled with electrophysiological experiments (French and Meisner 2007; Schuckel and French 2008). These methods indicate that linear, low-noise, wide frequency range control of odorant concentration could be realized in the olfactory stimulation. However, the odorant plume showed a radial distribution within the wind tunnel, indicating that a certain amount of turbulence occurred in the laminar flow when discharging the odor-laden air into the wind tunnel. At high wind speeds (ca., 1–1.5 m/s), the maximum frequency of odor concentration changes at the animal increased, together with the possibility of turbulence (Schuckel and French 2008). As in many studies, a filter paper impregnated with an odorant solution was used as the odor source. The actual odorant

concentration depends on the rate of evaporation from the filter paper, which is practically unknown (French and Meisner 2007).

In view of all the disadvantages of the methods used to date, we fabricated a novel odor stimulator based on the wind tunnel method. It can achieve laminar flow at low wind speeds (less than 0.8 m/s) while avoiding turbulent flow when the odor-laden air is discharged into laminar flow within the wind tunnel. Odor stimulation by laminar flow is expected to control the temporal pattern of odor concentration with high repeatability. We designed a stimulator in which the odor concentration can be controlled independently from the vapor pressure of the odorant chemicals.

Materials and methods

Overview and the operation of the stimulator

We fabricated a novel odor stimulator that stimulated insect olfaction in a controlled manner: 1) the odor concentration was maintained without fluctuation during the stimulation period, 2) the onset and cessation of odor stimulation were operated precisely and distinctly, and 3) the odor concentration of odor-laden air was controlled independently from the vapor pressure of the odorant chemicals.

The stimulator has 3 main parts: an odor conditioner, a Pitot tube, and a small wind tunnel (Figure 1). The odor conditioner comprises an odorant vaporizer with an external hot wire heater on the bottom and 2 glass syringes attached to the vaporizer. One syringe provides clean air to sweep odorant vapor out from the vaporizer. The other, with a motorized slide, sucks the odor-laden air to prepare the odor-conditioned sample air and then charges it into a Pitot tube. The Pitot tube, made from a glass pipette, was attached to the end of the odor conditioner and inserted into the wind tunnel. The tube opened downwind in the wind tunnel, so the sample air was released from the opening by suction resulting from the Bernoulli effect. These components were mutually connected mainly by Teflon tubes to prevent the possible adsorption of odorant chemicals. A Tygon tube was also used for flexibility. Valves were set between these components to change the flow path. A controller of the odor stimulator, which we designed and made, managed heating of the vaporizer, switching of valves, strokes of a syringe plunger, and the odor stimulation (Figure 1A).

The operation sequence of the stimulator is as follows (Figure 1B). 1) The given quantity of odorant chemicals in the vaporizer was evaporated by heating with the hot wire heater for 1 min. At that time, all the valves closed, so the odorant was vaporized into an aliquot of air (Figure 1B-1). 2) The valves at both sides of the vaporizer opened. Subsequently, the plunger of the sample-air syringe was pulled for 100 ml by the slide in 1.5 s. The plunger of the clean-air syringe was driven passively by the vacuum, accordingly. Shortly afterward, the valves set between the vaporizer and the sample-air syringe closed. In this process, unevenly distributed odorant gas in the vaporizer was diluted and homogenized with clean air to a given volume (160 ml) and reserved temporarily in the syringe. This process was conducted under airtight conditions (Figure 1B-2). 3) The valve between the sample-air syringe and the Pitot tube was opened. The plunger of the syringe was displaced for 7.0 ml to transfer sample air to the Pitot tube; then the valve closed again. Accordingly, sample air filled the Pitot tube while the excess amount was discarded into the wind tunnel (Figure 1B-3). 4) Sample air was introduced to the wind tunnel by suction through the Pitot tube only while its vent valve was open, so the onset and cessation of odor stimulation was operable by the opening and closing of the vent valve, respectively (Figure 1B-4). Details of the components are described below.

Odor conditioner

Vaporizer

The vaporizer consisted of a hot wire heater made of a Nichrome coil (wire, 0.3 mm outer diameter × 90 cm) and a heat chamber (78 ml glass flask) seated on the heater. Power (24 V DC) was automatically supplied to the heater from the controller according to the sequence program. The temperature at the bottom of the flask increased from 22 to 116 °C during the 1 min after the heater was turned on.

Valves

Four 2-way solenoid valves (USB-3-6-3B; CKD Corporation, Komaki, Japan) were used to change flow paths in the odor conditioner, one of which was also used as a vent valve to regulate odor stimulation.

Syringes and motorized slide

We used 2 glass syringes of ground finish (100 ml, #0601010; Tamano Co., Tokyo, Japan) to allow plungers to slide freely either by motion or by air suction. One syringe was mounted on a motorized linear slide driven by a stepping motor (S-Line SPB10V60-3P; Oriental Motor Co. Ltd, Tokyo, Japan). The stroke of the slide and that of the syringe plunger are regulated by the controller. The other syringe served as a reservoir to provide clean air into the closed air system of the odor conditioner.

Glass surface modification and heating

To prevent the influence of adsorption and/or condensation of odorant chemicals, 2 methods were applied: 1) surface silyl modification and 2) heating. 1) The inner surface of glassware used in the odor conditioners (i.e., the vaporizer and syringes) was treated with a silyl reagent: 10% *N,N*-Dimethylformamide solution of equivolumes of *1,1,1,3,3,3*-Hexamethyldisilazane and Trimethylchlorosilane (Tokyo Chemical Industry Co. Ltd, Tokyo, Japan). 2) During the experiments, the odor

conditioner was heated to 80 °C using a ribbon heater (JK-7; As ONE Corporation, Osaka, Japan), controlled using a thermostat (TKM-400; As ONE Corporation).

Wind tunnel

To ensure a sharp transition of odor states between presence and absence, together with a constant level of odor concentration during stimulation, we used a laminar flow with no turbulence to carry odor-laden "sample air" to the recording point. To produce a laminar flow, we fabricated a small wind tunnel using an acrylic tube (21.0 inner diameter [i.d.] × 235 mm) (Figure 2). The wind tunnel consisted of a flow straightener, a test section, a pressure buffer section, and a fan. The flow straightener was made of triple-layered 50-mesh polyester gauze sheets separated from each other by 7.0 mm.

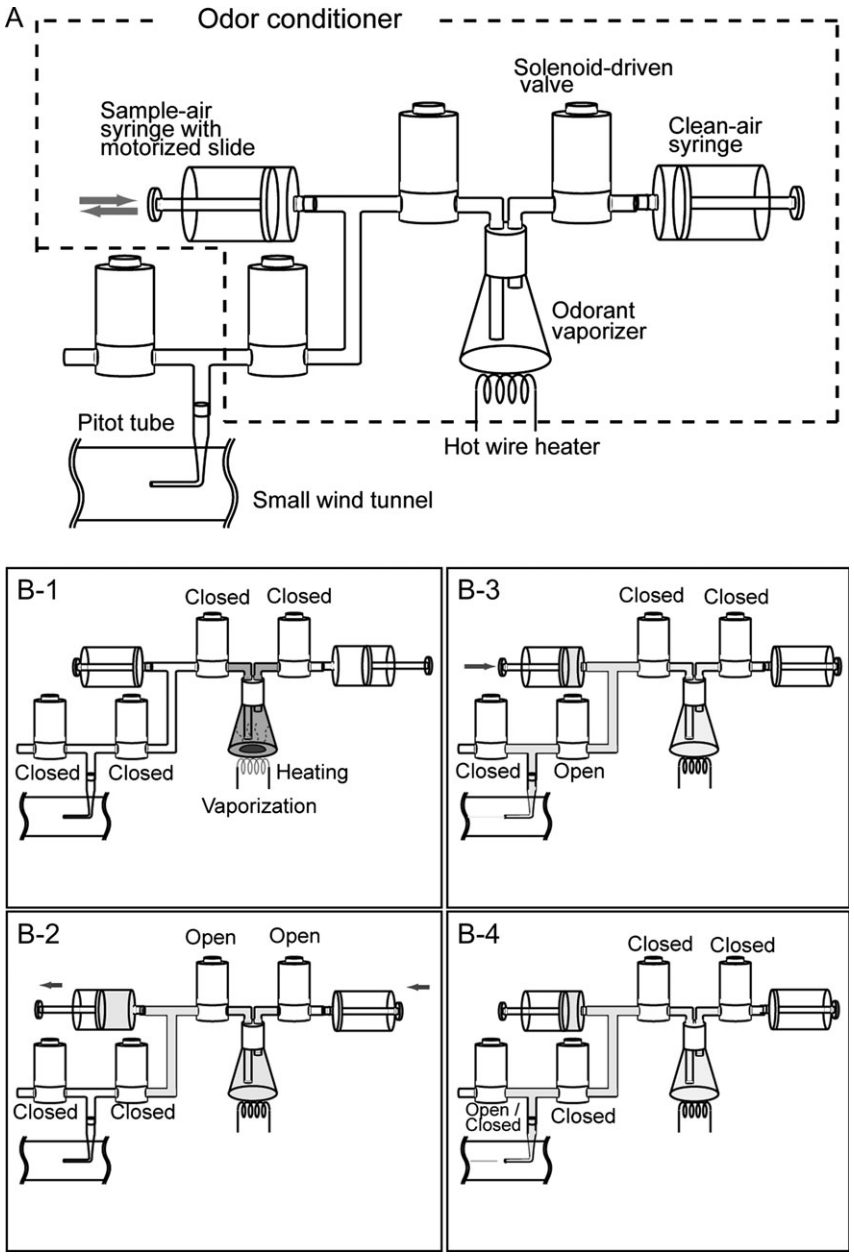

Figure 1 System overview and the odor stimulator operation. **(A)** Schematic drawing of the stimulator. **(B)** Motion sequence with valve status. The odorant chemical was vaporized by heating with a hot wire and odorant vapor filled the vaporizer (B-1). A motorized linear slide pulled the plunger of the sample-air syringe to introduce the odorant vapor into the syringe. The plunger of the clean-air syringe moved passively by suction. Then the air from the syringe swept the remaining odorant out from the vaporizer. Accordingly, odor-laden sample air with known concentration of odorant was prepared (B-2). The Pitot tube was charged with the sample air after a series of syringe operations (B-3). The sample air flowed into the wind tunnel by suction of the Bernoulli effect while the vent valve of the Pitot tube was open. Starting and stopping of odor stimulation was controlled through operation of the vent valve (B-4). Then the odor-laden sample air was discharged into the wind tunnel in a controlled manner.

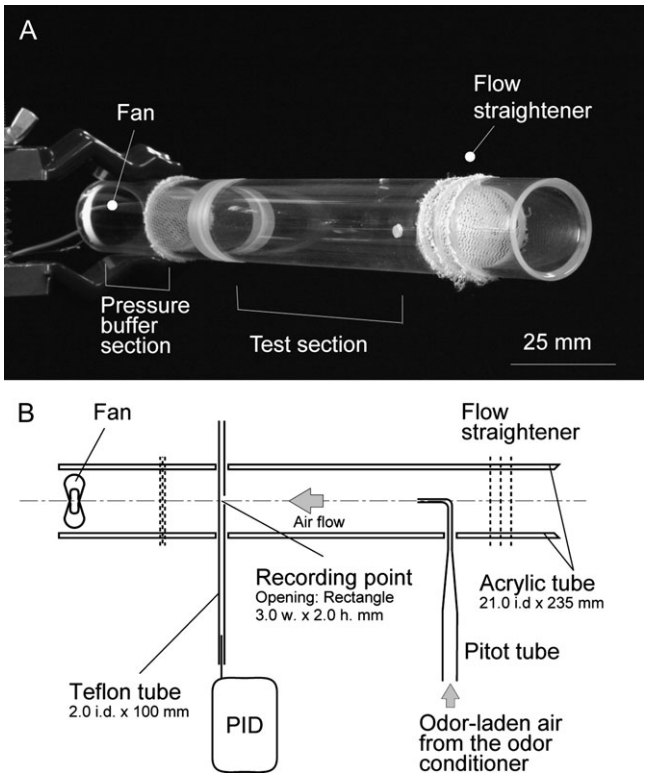

Figure 2 Structure and use of the wind tunnel. **(A)** A small wind tunnel made of acrylic. The wind tunnel was composed of a flow straightener, a test section, a pressure buffer, and a fan. **(B)** Plan view of the wind tunnel setup. Odor-laden air was discharged into the airflow from the Pitot tube located in the center of the acrylic tube. The PID sucked the odor-laden air through the Teflon tube. For experiments performed using insects, the insect antenna is placed at the Teflon tube position. The flow straightener and the pressure buffer were made from 50-mesh polyester gauze sheets (dotted lines).

The same sheets piled in 3 layers were used as the pressure buffer. Room air was introduced to the wind tunnel using a fan (Micro-jetfan, F2017AP-01WCV; SHICOH Co., Ltd, Yamato, Japan) plugged tightly into the bottom of the wind tunnel just downwind of the buffer section. The fan was driven by a DC power supply (AD-8723D; A and D Co., Ltd, Tokyo, Japan). Its voltage was monitored using an oscilloscope (SS-7804; Iwatsu Test Instruments Corporation, Tokyo, Japan) for regulation of the airflow speed to between 0.2 and 0.8 m/s. The area between the flow straightener and the buffer section was used as a test section. To discharge odor-laden air into the laminar flow, we used a Pitot tube with its opening aligned with the axis of the wind tunnel at 30 mm downwind from the flow straightener. The recording point of the odor concentration is at 40 mm downwind from the Pitot tube along the tunnel axis (Figure 2B). The exhaust from the wind tunnel was ventilated outside through a duct.

Stimulator controller

We operated the stimulation sequence under electrical control of a heater, 4 solenoid-driven valves, and a motorized slide using a peripheral interface controller (PIC, 16F84A; Microchip Technology Inc., Chandler, AZ). The operation sequence program, installed in the PIC, was developed using a compiler (PicBasic Pro ver. 2.47; Microtechnica, Tokyo, Japan). We made an electrical circuit to control 4 valves, 1 motorized slide, and a heat element using the PIC. Amplifier circuits were integrated in it for switching of the valves (24 V DC), positioning of the slide by pulse control (5 V DC, 3 channels), and for the power supply to the heating element of the vaporizer (24 V DC).

Flow analysis using high-speed video recording

To assess the wind tunnel performance, we visualized the odor plume of sample air in the wind tunnel using a titanium dioxide (TiO_2) smoke from a titanium tetrachloride ($TiCl_4$) droplet (Wako Pure Chemical Industries, Ltd, Osaka, Japan) in the Pitot tube. The smoke flowing out from the Pitot tube was recorded using a high-speed video camera (MotionScope M-1; Redlake Inc., Tucson, AZ). The recording was conducted at a framing rate of 250 frames per second with a shutter speed of 453 μs. The captured images were stored in memory for analyses. Using the digitizing program (Image Studio; Redlake Inc.), we verified the stability of the flow by measuring the variation in flow speeds, as well as the arrival time of the flow at the recording point, 40 mm downwind of the Pitot tube.

To measure the wind speed in the wind tunnel, we digitized the position of the smoke leading tip from the high-speed video recordings. Because the smoke discharged from the Pitot tube accelerated and reached constant speed before the recording point, the smoke speed at the recording point was regarded as the wind speed. We found the frame where the smoke tip was exactly at the recording point and then rewound for 3 frames (i.e., 12 ms) to measure the displacement of the smoke tip to calculate the wind speed. Applying 0.5–1.5 V as the wind tunnel fan power supply, we obtained the wind speed average and standard deviation (SD) for 19 different wind speeds. The arrival time from the discharge instant to the recording point was measured by counting the frames from the smoke appearance at the tip of the Pitot tube to the arrival to the recording point.

The plume shapes were also measured using a puff stimulation method for reference. A glass pipette, which was also used for the Pitot tube, was connected directly to a solenoid valve to regulate switching of the flow of cleaned air supplied from an air compressor (flow speed: 0.5 m/s). A filter paper (1 × 1 cm) impregnated with $TiCl_4$ was inserted in it, so the smoke comes out from the tip of the pipette as a puff when the valve opens.

Odor concentration measurement by a PID

We also measured temporal patterns of the odor concentration in the wind tunnel using a photoionization detector (mini-PID; Aurora Scientific Inc., Aurora, ON, Canada). A Teflon tube (2.0 i.d. × 100 mm) with an opening (3.0 mm

wide × 2.0 mm high) on its wall was connected to the sensor inlet of the detector. The tube was crossed through the wind tunnel via holes (3.0 mm i.d.) on the walls at both sides of the recording point at 40 mm downwind from the Pitot tube; it was placed with its center opening on the tunnel axis facing upwind (Figure 2B). To manage excessive sampling flow of the PID (675 ml/min), which might disturb laminar flow in the wind tunnel, the flow was split into 2 flows: one from the opening and the other from the open tip of the tube. This splitting of the flows caused, however, dilution of sampled air with fresh air from the open tip, so the odor concentration detected using the PID displayed a lower concentration according to the dilution ratio.

The concentration data were logged using a data acquisition module (USB-9215A; National Instruments Corporation, Austin, TX) at 333 Hz. The data were then stored in a computer for additional analyses using software program (LabVIEW; National Instruments Corporation) running on a widely used computer operating system (Windows XP; Microsoft Corporation, Redmond, WA).

Odorants

We used 2 chemicals with different boiling points (b.p.) as odorants: 2-heptanone (b.p.: 151 °C; Wako Pure Chemical Industries, Ltd) and linalool (b.p.: 200 °C; Tokyo Chemical Industry Co., Ltd.) in the odor concentration measurement test. 2-Heptanone had a sufficiently low ionization energy of 9.18 eV (Ashmore and Burgess 1978) to be ionized by the PID used for this study (maximum ionized energy of 10.6 eV). Although the ionization energy of linalool is not known, the signal detection by PID was confirmed. These chemicals were applied into the vaporizer flask as neat liquid.

Cleaning of the odor conditioner

The odor conditioner (Figure 1) was cleaned by flushing solvent methanol after each experiment to avoid odor contamination. The clean-air syringe (Figure 1) was loaded with 100 ml of methanol instead of clean air. All the valves and syringes were operated in the same sequential process as in the odor conditioning experiment with the heater turned off

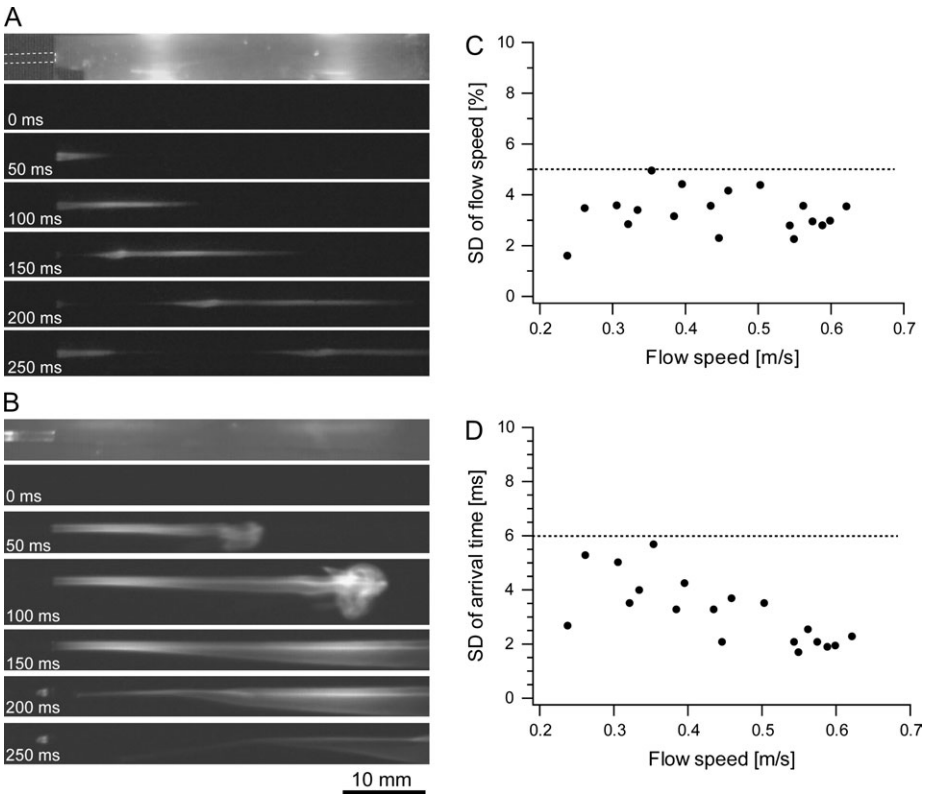

Figure 3 Flow analysis. **(A)** An odor plume generated from a Pitot tube in the wind tunnel. The odor plume, marked by TiO_2 smoke, extended in a thin, straight line form with almost no turbulence. Images after discharge were processed to highlight the smoke, except for a raw image at the top. The position of the Pitot tube is shown in dotted lines. The elapsed time is shown on the left side. **(B)** A puff of an odor plume. The plume, changing its shape temporarily, brought large turbulence in front. **(C)** Variation of the flow speed at the recording point. Each point represents the variation of flow speed given as a percentage of the SD to the mean (N = 10). The variations were examined at 19 airflow speeds of 0.22–0.62 m/s by regulating a power supply to the fan. Throughout the range, the maximum variation in the range was 4.9%, indicating that the wind tunnel produced laminar flow with high stability. **(D)** Variation of arrival time at the recording point. The same records were analyzed for the time of odor arrival at the recording point, equivalent to the delay of odor stimulation. The SDs of the arrival time did not become greater than 6.0 ms, implying the accuracy of the odor stimulator.

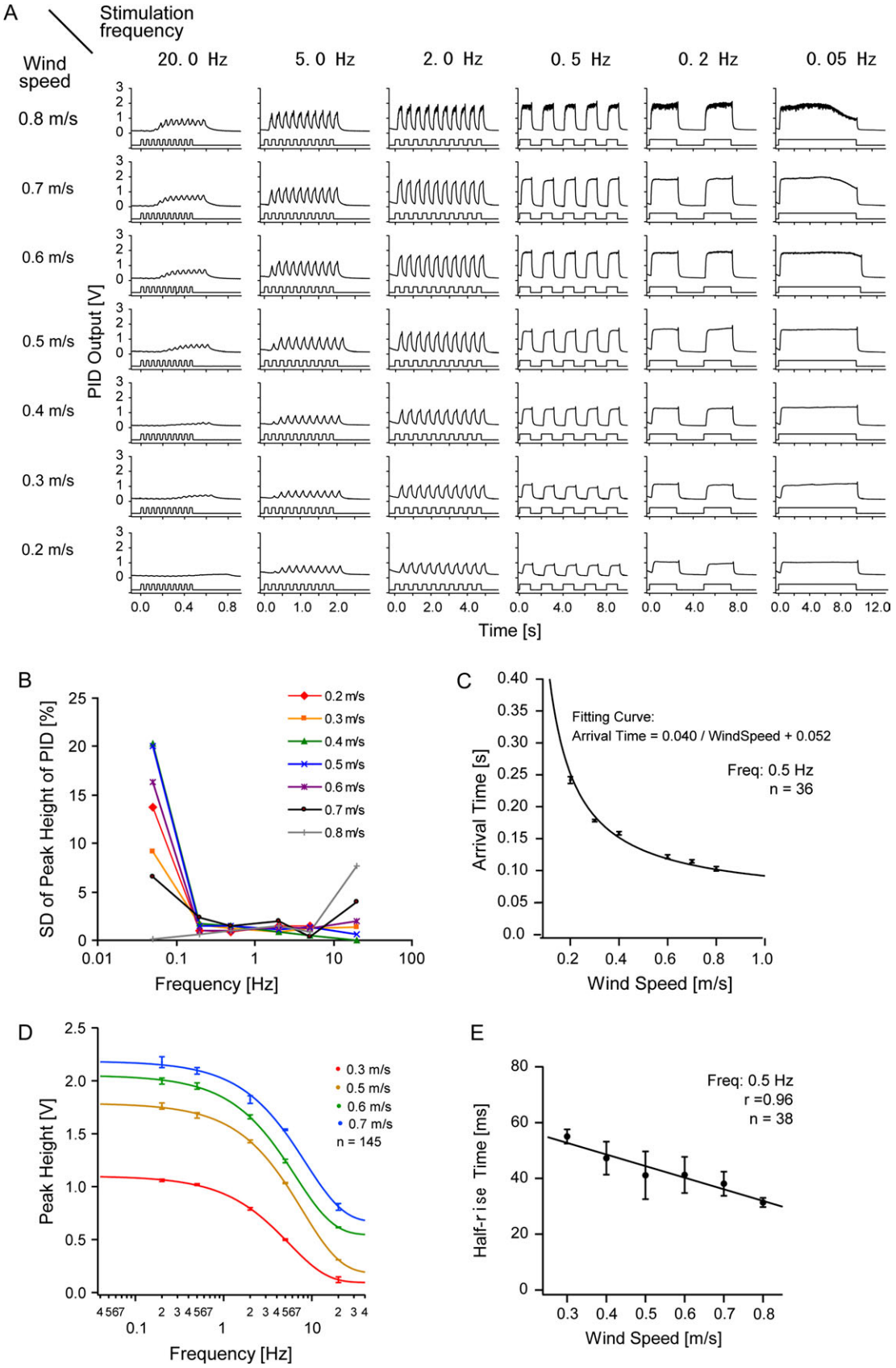

(Figure 1). After the solvent was exhausted via a plastic tube connected to the base of the Pitot tube, the clean-air syringe was removed and a clean airflow (10 l/min) from an air compressor blew the remaining solvent off from the odor conditioner for 15 min.

Results

Verification of a laminar flow in the wind tunnel

We examined the stability of the flow in the wind tunnel by marking the flow with TiO_2 smoke. The smoke, discharged from the Pitot tube into the wind tunnel, formed a straight line shape within the test section indicating the homogeneity of the flow (Figure 3A). By contrast, in the puff stimulation, smoke showed apparent heterogeneity. Figure 3B depicts that the smoke flow contained many vortices. The shape of the smoke changed temporarily.

Validity of flow speed control in the wind tunnel

To verify the stability of the flow, we measured the speed of the airflow from the displacement of a smoke image at the recording point (Figure 3C). The airflow speed was changed by shifting the voltage of DC power supply to the fan, so we measured the speed at 19 points in a series of voltages. From the replicated results at each voltage point ($N = 10$), the variation of flow speed was calculated as a percentage of the SD to the mean (Figure 3C). The results indicated that the variance of the airflow speed was less than 4.94% (mean 3.2%), suggesting that the flow in the wind tunnel was highly stable and reproducible. The same records were analyzed for the time of odor arrival at the recording point, which is the actual onset of the stimulation (Figure 3D). The variation of the arrival time did not become greater than 6.0 ms, meaning that the accuracy of odor stimulation was within 6.0 ms for all examined flow speeds (0.2–0.7 m/s).

Temporal pattern of odor concentration

We examined the temporal pattern of the concentration of the odorant discharged from a Pitot tube. The sample air was prepared from 1.0 µl of 2-heptanone vaporized and diluted into 160 ml of clean air in the conditioner. The odor concentration at the recording point of the wind tunnel was measured using the PID. Figure 4A shows the PID output representing the temporal changes in odor concentration (the top trace in each graph) and the timing of the vent valve opening (the bottom trace). The average and SD of peak heights of the PID output were calculated from 6 trials under the same wind speed and frequency conditions. Percentages of SDs for the height averages 0.05–20 Hz are shown for each wind speed (i.e., 0.2–0.8 m/s) in Figure 4B. The SDs of the height averages showed less than 2.4% within 0.2–2.0 Hz frequency range. Using the PID, we measured the actual arrival time, defined as the time from the onset of vent valve opening to the onset of output signal rising of the PID in each wind speed. As it was evident that the arrival time was independent from frequency, we arbitrarily used the 0.5-Hz condition (Figure 4C). We fitted the following curve for the wind speed versus arrival time

$$T = l/v + 0.052, \quad (1)$$

where T is the arrival time, l is the distance from the tip of the Pitot tube to the recording point (0.04 m), and v is the wind speed. Equation (1) shows that the system includes basal delay of 52 ms.

The relation between the frequency and peak height of PID outputs is shown in Figure 4D. For 0.2–0.5 Hz, the peak heights remained at a 90% level or more at each wind speed (0.3, 0.5, 0.6, and 0.7 m/s), which suggests that the maximum frequency for practical use was 0.5 Hz. The time constants represented as half-rise times of the output at 0.5 Hz are shown for each wind speed in Figure 4E. The half-rise time decreased concomitantly with increasing wind speed. The minimum was 31 ± 1.6 ms SD at 0.8 m/s wind speed and maximum was 55.0 ± 2.5 ms SD at 0.3 m/s wind speed.

Effects of glass surface modification and heating

The final concentration of the odor-laden air at the entrance of the Pitot tube was compared with the initial concentration of the odor-laden air generated in the vaporizer (see Figure 1). The final and the initial concentrations were prepared from either 1.0 µl of 2-heptanone or linalool vaporized into 160 ml of air. The odor concentrations were measured by sampling the air with the PID by suction at 675 ml/min. To examine adsorption and/or condensation effects of odorant chemicals, we compared the final concentrations with the initial in all the combinations of glass surface silyl-modified (S+), unmodified (S–), heated (H+), and unheated (H–) conditions (Figure 5). For 2-heptanone, PID output for the initial concentration was 7.2 V, where the vaporizer was silyl modified and heated (S+, H+). Unmodified and unheated

Figure 4 The temporal pattern of the odor concentration in the wind tunnel for 2-heptanone. **(A)** The graph matrix of the concentration pattern in the wind tunnel. In each graph, the top trace represents the PID output and the bottom trace represents the stimulation timing. Rows in the matrix show wind speed and columns show the stimulation frequency. The concentration of an airborne odorant was measured at 40 mm downwind of the Pitot tube using a PID. **(B)** Variability in the peak height of the PID output. The percentages of SDs of the peak height from 6 repeated trials are shown for each point. For frequencies of 0.2–5 Hz, the maximum error was 2.4%. **(C)** The curve of wind speed versus arrival time measured from the onset of stimulation to onset of PID output rising at 0.5 Hz. **(D)** Frequency response of the peak height of the PID outputs. **(E)** Half-rise time of the temporal pattern of the odor concentration. Increasing the wind speed reduces the half-rise time.

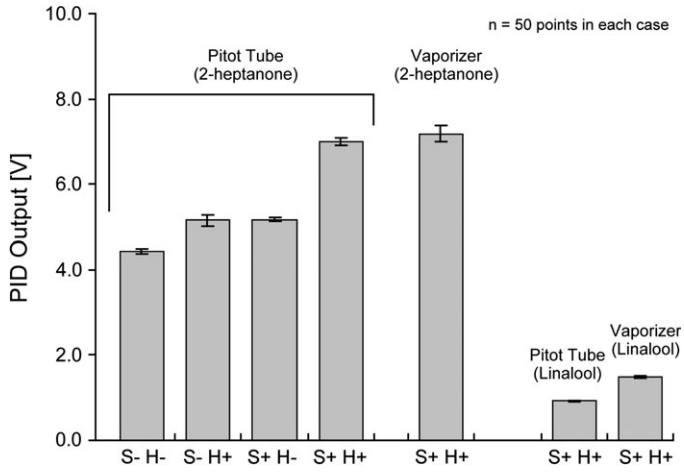

Figure 5 The loss of odor concentration in the odor conditioner with silyl modification and/or heating. Treatments of the glassware surface were silyl modified (S+), unmodified (S−), heating during test (H+), and unheated (H−). For heating of the silyl-modified surface (S+, H+ condition), the odor concentration in the Pitot tube shows 97.4% of 2-heptanone from the initial concentration in the vaporizer. In the case of linalool, the concentration in the Pitot tube showed only 62.0% (See Discussion).

conditions (S–, H–) showed 4.4 V to the final concentration, which is 61.8% of the initial concentration. Under (S–, H+) and (S+, H–) conditions, the final concentration, respectively, showed 71.8% and 71.9% to the initial concentration. At (S+, H+) condition, the PID output of the final concentration was almost identical to the initial concentration (97.4%). The same combinations (S+, H+) were examined also for linalool. In this case, the final concentration showed 62.0% of the initial concentration.

Discussion

We fabricated an odor stimulator that can regulate the temporal pattern of odor concentration precisely with low wind speeds (0.2–0.8 m/s). The wind tunnel of the stimulator produced laminar flow with a SD of the wind speed of less than 4.9% (Figure 3A and C). The onset of the stimulation was controllable to 6 ms precision (Figure 3D). The temporal patterns in concentrations showed high repeatability because the peak concentrations during stimulation were duplicated in each trial with only a 2.4% error margin (Figure 4B). The concentration showed a rapid change with less than 55 ms of half-rise time (Figure 4E). Consequently, the controlled exposure of a test animal to an airborne odor was achieved with millisecond-order precision.

Selection of flow speed in this wind tunnel method required a compromise between several factors. Within the low wind speed range (0.2–0.8 m/s), the frequency response of stimulation was slow (0.5 Hz at 90% of maximum concentration level) (Figure 4D). Increased wind speeds reduced the arrival time and the half-rise time, and it increased the maximum useful frequency at which odorant concentration in single pulses reached a stable level (Figure 4C–E). It also increases, however, the possibility of turbulence occurring in the airflow in the wind tunnel. We chose a low wind speed range to achieve a high accuracy and repeatability of the temporal concentration pattern of the stimulation.

In the stimulator, the odor concentration was regulated irrespective of its partial pressure and ambient temperature because all the given amount of odorant material was forced to vaporize by heat and then diluted using a known volume of air in the odor conditioner. In an airtight condition, the adsorption and condensation of the material on the inner walls of the apparatus can be affected by the initial concentration of the material, vapor pressure, temperature of the inner wall surface and/or the diluting air, etc. To avoid these effects, we applied silyl modification of a glass surface and heating of the odor conditioner. These techniques were the same as those applied in gas chromatography instruments.

Applying these methods, the final concentration in the sample air was 97.4% of that generated in the vaporizer in the case of 2-heptanone, showing a minimum loss attributable to adsorption and condensation. However, for linalool, the final concentration of the sample air was as low as 62.0% from the initial concentration generated in the vaporizer. We consider that this difference between the case of 2-heptanone and linalool is attributable to the higher b.p. of linalool (200 °C) than that of 2-heptanone (151 °C). Because linalool has a higher b.p., it presumably shows stronger adsorption and condensation on the inner wall of the apparatus. We were unable to determine, however, the absolute concentration in the odor-laden air of the wind tunnel because we have no evidence that all the odorant solution was vaporized and then retained in the air in the vaporizer with no adsorption or condensation. In reality, the odor concentration of a stimulus can be estimated as a sufficient approximation at least for odorant chemicals having a low b.p., as 2-heptanone has.

As a following step, we are planning to measure neural responses from the antennal lobe in the American cockroach (*Periplaneta americana*) using the stimulator. We expect to obtain the information processing time, defined as the elapsed time from the stimulus onset to the neural activation in the antennal lobe.

Funding

Japan Society for the Promotion of Science, 21st COE: 21st Century Center of Excellence program.

Acknowledgements

We thank Dr Pablo J. Perez Goodwyn for comments and suggestions about the article.

References

Arabzadeh E, Zorzin E, Diamond ME. 2005. Neuronal encoding of texture in the whisker sensory pathway. PLoS Biol. 3:E17.

Ashmore FS, Burgess AR. 1978. Photoelectron spectra of the unbranched C_5-C_7 alkenes, aldehydes and ketones. J Chem Soc Faraday Trans. 74:734–742.

Baker TC, Hansson BS, Löfstedt C, Löfqvist J. 1988. Adaptation of antennal neurons in moths is associated with cessation of pheromone-mediated upwind flight. Proc Natl Acad Sci USA. 85:9826–9830.

Barrozo RB, Kaissling KE. 2002. Repetitive stimulation of olfactory receptor cells in female silkmoths *Bombyx mori L*. J Insect Physiol. 48:825–834.

Brown LS, Joseph J, Stopfer M. 2005. Encoding a temporally structured stimulus with a temporally structured neural representation. Nat Neurosci. 8:1568–1576.

Christensen TA, Heinbockel T, Hildebrand JG. 1996. Olfactory information processing in the brain: encoding chemical and temporal features of odors. J Neurobiol. 30:82–91.

Christensen TA, Pawlowski VM, Lei H, Hildebrand JG. 2000. Multi-unit recordings reveal context-dependent modulation of synchrony in odor-specific neural ensembles. Nat Neurosci. 9:927–931.

French AS, Meisner S. 2007. A new method for wide frequency range dynamic olfactory stimulation and characterization. Chem Senses. 32:681–688.

Fuster JM, Jervey JP. 1982. Neuronal firing in the inferotemporal cortex of the monkey in a visual memory task. J Neurosci. 2:361–375.

Hamilton KA, Kauer JS. 1988. Responses of mitral/tufted cells to orthodromic and antidomic electrical stimulation in the olfactory bulb of the tiger salamander. J Neurophysiol. 59:1736–1755.

Heinbockel T, Christensen TA, Hildebrand JG. 1999. Temporal tuning of odor responses in pheromone-responsive projection neurons in the brain of the sphinx moth *Manduca sexta*. J Comp Neurol. 409:1–12.

Jones LM, Depireux DA, Simons DJ, Keller A. 2004. Robust temporal coding in the trigeminal system. Science. 304:1986–1989.

Laurent G, Davidowitz H. 1994. Encoding of olfactory information with oscillating neural assemblies. Science. 265:1872–1875.

Lei H, Christensen TA, Hildebrand JG. 2004. Spatial and temporal organization of ensemble representations for different odor classes in the moth antennal lobe. J Neurosci. 24:11108–11119.

Machens CK, Stemmler MB, Prinz P, Krahe R, Ronacher B, Herz AV. 2001. Representation of acoustic communication signals by insect auditory receptor neurons. J Neurosci. 21:3215–3227.

Mafra-Neto A, Cardé RT. 1995. Influence of plume structure and pheromone concentration on upwind flight of *Cadra cautella* males. Physiol Entomol. 20:117–133.

Meister M. 1996. Multineuronal codes in retinal signaling. Proc Natl Acad Sci USA. 93:609–614.

Nagarajan SS, Cheung SW, Bedenbaugh P, Beitel RE, Schreiner CE, Merzenich MM. 2002. Representation of spectral and temporal envelope of twitter vocalizations in common marmoset primary auditory cortex. J Neurophysiol. 87:1723–1737.

Schuckel J, French AS. 2008. A digital sequence method of dynamic olfactory characterization. J Neurosci Methods. 171:98–103.

Stopfer M, Jayaraman V, Laurent G. 2003. Intensity versus identity coding in an olfactory system. Neuron. 39:991–1004.

Vetter RS, Sage AE, Justus KA, Cardé RT, Galizia CG. 2006. Temporal integrity of an airborne odor stimulus is greatly affected by physical aspects of the odor delivery system. Chem Senses. 31:359–369.

Vickers NJ, Christensen TA, Baker TC, Hildebrand JG. 2001. Odour-plume dynamics influence the brain's olfactory code. Nature. 410:466–470.

Wehr M, Laurent G. 1996. Odour encoding by temporal sequences of firing in oscillating neural assemblies. Nature. 384:162–166.

Willis MA, Baker TC. 1984. Effects of intermittent and continuous pheromone stimulation on the flight behavior of the oriental fruit moth, *Grapholita molesta*. Physiol Entomol. 9:341–358.

Accepted March 12, 2009